Yardney Technical Products, Inc.
82 Mechanic Street
Pawcatuck, CT 06379
TEL: 860/599-1100
FAX: 860/599-3903; 5122

Composite, Nanoparticle-Based Anode Materials for Li-Ion Batteries Applied in Hybrid Electric Vehicles (HEVs)

Final Report

Phase I STTR Grant # DE-FG02-07ER86332
Department of Energy, Basic Energy Science Topic 10d

Principle Investigator: Malgorzata K. Gulbinska

Table of Contents

1. Significance, Background Information and Technical Approach

1.1 Identification and Significance of the Problem or Opportunity, and Technical Approach

1.1.1 Introduction

Lithium-ion batteries are promising energy storage devices in hybrid and electric vehicles with high specific energy values (~150 Wh/kg), energy density (~400 Wh/L), and long cycle life (>15 years*). However, applications in hybrid and electric vehicles require increased energy density and improved low-temperature (<–10° C) performance. Silicon-based anodes are inexpensive, environmentally benign, and offer excellent theoretical capacity values (~4000 mAh/g),[1] leading to significantly less anode material and thus increasing the overall energy density value for the complete battery (>500 Wh/L). However, tremendous volume changes occur during cycling of pure silicon-based anodes. The expansion and contraction of these silicon particles causes them to fracture and lose electrical contact to the current collector ultimately severely limiting their cycle life. In Phase I of this project *Yardney Technical Products, Inc.*** proposed development of a carbon/nano-silicon composite anode material with improved energy density and silicon's cycleability.

In the carbon/nano-Si composite, silicon nanoparticles were embedded in a partially-graphitized carbonaceous matrix. The cycle life of anode material would be extended by decreasing the average particle size of active material (silicon) and by encapsulation of silicon nanoparticles in a ductile carbonaceous matrix. Decreasing the average particle size to a nano-region would also shorten Li-ion diffusion path and thus improve rate capability of the silicon-based anodes. Improved chemical inertness towards PC-based, low-temperature electrolytes was expected as an additional benefit of a thin, partially graphitized coating around the active electrode material.

1.1.2 Background Information

Increasing the energy density of a lithium-ion battery can be accomplished by improving the energy density values of its electrodes, and/or by modifying the battery design to use lightweight, non-electrochemically active components (such as the battery casing). In Phase I of this project, we developed and characterized nanoparticle-sized silicon composite anode materials with high specific capacity values.

* Cycle life depends on details of the battery design, and the cycling load profile

** Later referred to as *Yardney*

Silicon based materials have been extensively studied as a potential anode material to replace carbonaceous materials because of its high specific energy (~4000 mAh/g versus 372 mAh/g for carbon). While silicon is capable of reversibly cycling lithium, its cycle life is limited because of extreme volume changes as it charged and discharged. These volume changes lead to particle fracture, which can cause them to lose electrical contact with the current collector and hence loss of capacity and low cycle life. Potential solutions to solve this mechanical instability problem include decreasing the particle size and/or incorporating silicon within a ductile Li-ion conducting matrix.[2] Because the stress caused by the expansion and contraction the particle during cycling is related to its size, smaller particles should have less stress and less fracturing of the particles. Nanoparticles of silicon should, therefore, make an ideal candidate for a high energy density anode material. However, the use of nanoparticles for the anode introduces other problems. One of these problems is caused by their extremely high surface area of the nanoparticles-based electrode that leads to a very high irreversible capacity. This is due to a large amount of lithium being consumed during the first charge forming the SEI (solid electrolyte interface) layer on the anode surface. A second problem with nanoparticle materials is the large amount of binder required, which leads to poor electrical contact between the current collector and particles that limits rate capability. Furthermore, increased amount of binder translates to lower capacity due to the high amount of inactive material. Ikeda *et al*.[3] reported the use of a copper foil anode current collector with the increased surface roughness for the enhanced silicon coating-to-foil electrical contact. In order to evaluate benefits of the enhanced adhesion of the active material coating to the current collecting foil, as part of the Phase II effort *Yardney* will prepare the electrolytic copper foil with roughened surface processed in a similar manner to the current collector used by Ikeda *et al*. In Phase I research, our standard copper foil current collector was used.

1.1.3 Technical Approach

1.1.3.1 Basic concept

In an effort to develop a high energy density anode with high cycle life, we proposed to develop a graphite/nanoparticle silicon/carbon composite anode. The new composite anode material will consist of the graphitic core, surrounded by nano-dispersed silicon nanoparticles, embedded in an outer layer of partially graphitized carbon matrix (Figure 1). Because nanoparticles of silicon are contained within a large carbonaceous matrix with low surface area, the irreversible capacity problems associated with nanoparticles would be avoided while taking advantage of the high energy density of silicon. The carbonaceous matrix containing the silicon nanoparticles was similar to the carbon currently used in Li-ion cells and may contribute to the capacity of the anode. Graphite, which was the composite's core and "scaffolding", possessed good theoretical lithium intercalation specific capacity of 372 mAh/g, flat voltage potential profile, and long cycle life.

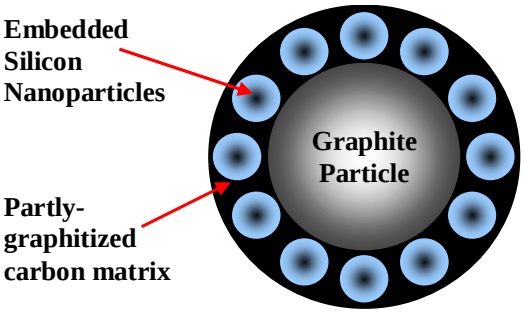

Figure 1. Schematic of the proposed graphite/silicon/carbon composite anode material

The layer of nano-dispersed silicon particles would increase specific capacity of the composite anode (Figure 2), beyond the capacity of carbon alone. The specific capacity of these composite anodes was estimated between that of silicon (4000 mAh/g) and graphite (372 mAh/g) and would depend upon how many silicon nanoparticles can be placed around a graphite particle. The outermost component of the proposed composite is a partially graphitized conductive carbon matrix. This carbonaceous layer performed several functions: it sustained the electrical contact between the electrode material and the current collector, immobilized dispersed silicon nanoparticles, and decreased the total electrode surface area. Since the large surface area that is common in nanoparticles is the cause for their large irreversible capacity values, we expect a beneficial effect from the decreased surface area that results from coating the nanoparticles. Furthermore, the partially graphitized carbon of the outer sphere is expected to be more tolerant to PC containing electrolyte systems than graphitic carbon, which may allow the use of this solvent that could offer advantages at low temperatures.

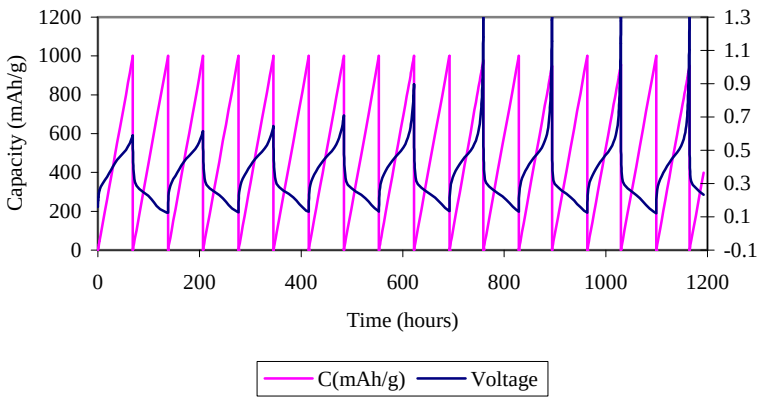

Figure 2. Li/carbon coated silicon cell with the capacity cutoff of 1000 mAh/g, in the voltage range of 0.01 to 1.3 volts

Another potential advantage of the nano-composite anodes is that a lower amount of conductive carbon black may be used because the outer surface of the composite particles is highly conductive. Conductive carbon black additives are commonly used in Li-ion electrodes to increase cycle life and decrease polarization of the electrode and to provide good electronic contact between the electrode particles and the current collector. However, even small amounts of carbon additive (our normal anode coating has 3% of a conductive diluent) result in lower volumetric energy density of composite electrodes.

So that neither energy, nor power density are compromised, the carbon quality, content and distribution in composite electrodes need to be optimized. The larger the ratio of sp^2-coordinated carbon (excellent electronic conductor) to disordered sp^3-coordinated carbonaceous materials (poor electronic conductors); the better is the electrochemical utilization of the electrode.[4]

We employed the Chemical Vapor Deposition (CVD) of carbon coating onto silicon nanoparticles to produce a thin carbonaceous matrix. Chemical vapor deposition of films and coatings involve the chemical reactions of gaseous reactants on or near the vicinity of a heated substrate surface.[5] We deposited the carbon coating from hydrocarbon (C_nH_{2n}) precursor in a high-temperature furnace at 900ºC onto the silicon powder substrate. The vapor phase process allows the deposition of a smooth continuous film of carbon, as thin as a few monolayers. Furthermore, since it is a gas–solid reaction, the gas can penetrate and coat inner pore areas of the powder. By employing the CVD method in coating of the silicon particles, we expected to decrease the total amount of carbon needed for enhanced electronic conductivity of the active material, or perhaps entirely avoid adding the extra conductive carbonaceous diluents to the anode slurry. We tested the CVD-derived C/Si composite's performance in coin half cells (against lithium metal) and in full coin cells, against our standard $LiNi_{0.8}Co_{0.2}O_2$ cathodes.

As a second carbon deposition method, we proposed to use a microwave-assisted carbon coating process. Microwave irradiation offers a facile, inexpensive, and clean carbon coating synthesis method through low-temperature pyrolysis of organic precursors, often resulting in higher yields and shorter reaction times when compared with conventional heating methods. Microwave-assisted_deposition of carbon coating should yield larger ratio of sp^2-coordinated carbon (excellent electronic conductor) to disordered or sp^3-coordinated carbonaceous materials (poor electronic conductors), and consequently better electrochemical utilization of anode.[6] The microwave-derived carbonaceous layer was partially graphitized and therefore highly conductive, also resulting in a decreased amount of conductive additives. The electrochemical performance in coin cells of the respective CVD-coated and the MW-irradiated C/Si composites was compared against the baseline of our standard carbonaceous anode, based on the Meso Carbon Micro Beads (MCMB) material.

1.2 Anticipated Public Benefits

Lithium-ion cells with the improved energy density and capacity, without sacrificing the cycle life, are of great interest for many civilian and military applications such as electric and hybrid vehicles, satellites, aircraft, portable power tools, electronic news gathering cameras, portable medical equipment and other similar applications. The proposed technology will improve the specific energy and energy density of Li-ion batteries. This will benefit many areas that use battery technology and could help open new markets for this technology. Hybrid and electric automobiles, which have come on the market and have been extremely successful, especially with recent increase in energy prices, will benefit from this technology. Consumer electronics such as notebook computers, cameras, and cell phones among other applications would benefit from an increased battery capacity that this program will develop. The proposed technology should also benefit military and aerospace applications. It is also hoped that the materials developed in this program will be more tolerant to propylene carbonate (PC), which may help improve the low temperature performance of these batteries. This will further help applications where the ambient temperature may not be controlled, such as in automobile, aerospace and military applications.

1.3 Degree to which Phase I has Demonstrated Technical Feasibility

1.3.1 Purpose of the Phase I Research

The main purpose of this Phase I research was to demonstrate the technical feasibility of syntheses and applications of silicon-based anodes in lithium-ion batteries. We proposed to achieve this goal by focused syntheses and testing of several generations of silicon/carbon-based materials. Two parallel research effort strains were conducted in Phase I:

- Part of research focused on the development of the chemical-vapor deposition (CVD) methods of coating silicon substrates with a uniform carbon coating. This research effort was pursued at the University of Connecticut. The syntheses at University of Connecticut were focused on the vapor deposition parameters control and physical analyses (e.g.: SEM, Raman spectroscopy) of coated materials. The silicon wafers with various orientations were used to test carbon deposition onto different crystallographic planes of silicon. Several hydrocarbons were used as carbon precursors and a temperature effect on coating quality was investigated
- The industrial part of research took place at *Yardney Technical Products, Inc*. where we employed the already existing CVD apparatus and the microwave oven set-up to pursue the syntheses of coin cell-destined anode materials. Our task at Yardney was to electrochemically test the silicon-based materials and screen the anode powders for the best cell performance. The goal of this part of research was to obtain reproducibly coated silicon powder-based samples in amounts appropriate for initial coin cell testing (~10 g each batch).

1.3.2 Technical Objectives of the Phase I Research

The following technical objectives have been identified in order to fulfill the purpose of the Phase I of this project:

Objective 1. Prepare graphite/silicon/carbon composite anode materials.

Objective 2. Characterize synthesized anode materials.

Objective 3. Test and evaluate performance of the anodes in half-cells and full cells.

Objective 4. Correlate performance to matrix graphitization degree, silicon nanoparticle content and conductivity and screen the best active material candidates.

1.3.3 Summary of Technical Tasks set in Phase I Research

A list of tasks was compiled in order to meet the objectives of the Phase I of this project. The task outline that was defined for Phase I is presented in Table 1. Individual tasks are discussed in greater detail in Section 1.3.4. The degree to which each individual technical objective was met is discussed in Section 1.3.6 and Section 1.3.7. Several technical questions were formulated at the beginning of the Phase I work and our proposed answers are presented in Section 1.3.6.1.

Table 1. Task outline

Task	Task Description	Task Performed By	Comment
1	*Carbon Coating by **CVD Method***	*UConn + Yardney*	*Tasks 1-2 Fall into the **Materials Preparation** Category.*
2	*Carbon Coating via the **MW-Assisted Method***	*UConn + Yardney*	
3	***Physical Analyses** of the Synthesized Materials*	*UConn*	-
4	***Preliminary** Coin Cell Evaluation of Anodes*	*Yardney*	***Half-Coin** Cells **Formation***
5	***In-Depth** Anode **Half-Cell** Cycling*	*Yardney*	-
6	***In-Depth Full-Cell** Cycling*	*Yardney*	-
7	*Final Report Submittal*	*Yardney + UConn*	*Summary of Tasks 1-6*

1.3.4 Research Carried Out in Phase I

This section describes each task that was performed during the Phase I research in detail.

1.3.4.1 Synthetic approach

Task 1. CVD-assisted syntheses of graphite/silicon/carbon composite anode materials

The synthesis of the graphite/nanoparticle silicon/carbon composite was partially performed at the *University of Connecticut* (initial experiments and optimization of experimental conditions) and then at *Yardney Technical Products, Inc.* (synthetic scale-up). Milled silicon nanoparticles (*Union Process*, Chicago, IL) were placed in the CVD reactor. Carbon coating will be deposited from hydrocarbon (*Airgas*) precursor in a high-temperature furnace at 900ºC onto the silicon powder substrate. Chemical vapor deposition involves the dissociation and/or chemical reactions of gaseous reactants in an activated (heat, light, plasma) environment, followed by the formation of a stable solid product. We deposited the carbon coating from hydrocarbon (C_nH_{2n}) precursor (mixed with Ar gas) in a high-temperature furnace at 900ºC onto the silicon powder substrate. A schematic of the CVD process is given in Figure 3.

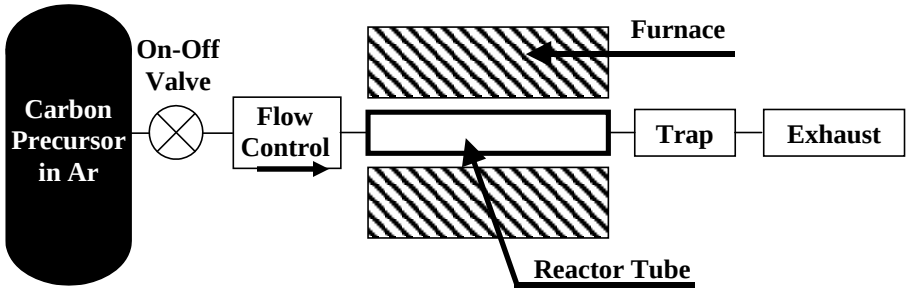

Figure 3. Schematic of the CVD apparatus

Task 2. Microwave-assisted syntheses of graphite/silicon/carbon composite anode materials

The syntheses of the graphite/nanoparticle silicon/carbon composite was in part performed at Steven L. Suib's lab at the *Chemistry Department* of *University of Connecticut*[***] (initial experiments and optimization of experimental conditions) and then at *Yardney Technical Products, Inc.* (synthetic scale-up). We initially attempted the MW-assisted carbon deposition method that consisted of the following steps:

- ***Step 1:*** *Reagent mixing and sonication.* This step distributed the silicon nanoparticles around the surface of the larger graphite particles. Graphite particles were mixed thoroughly with the silicon nanoparticles and the liquid hydrocarbon precursor (e.g. toluene). However, nanoparticulate powders often agglomerate via van der Waals forces and by hydrogen bonding in order to minimize their high surface area and the interfacial energy. Agglomeration of particles may occur during synthesis, drying, handling, and processing (Figure 4). Deagglomeration was achieved by sonication (Figure 5) in an appropriate solvent.[7,8] for about 1-10 minutes. It was expected that the silicon nanoparticles then would collect around the surface of the larger particles (in this case, the graphite).
- ***Step 2:*** *Removal of the excess hydrocarbon precursor.* Excess toluene was evaporated at room temperature, under mild vacuum (~30 in Hg vacuum). This stage would yield the graphite particles covered with a thin layer of adsorbed toluene containing well-dispersed silicon nanoparticles.

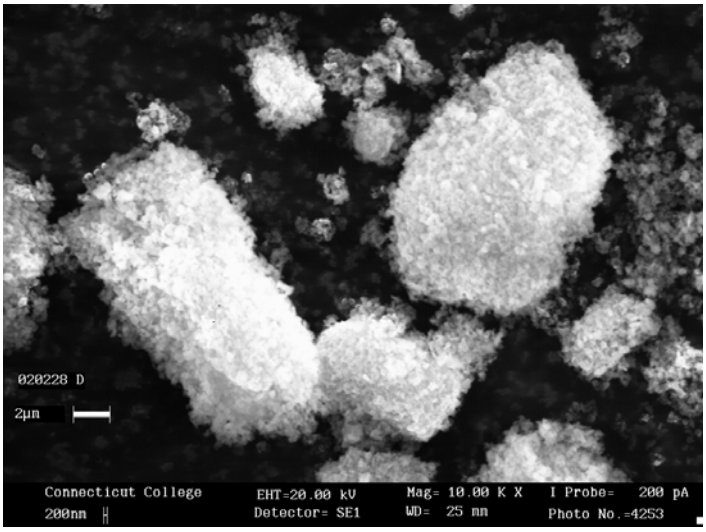

Figure 4. SEM micrograph of the milled, re-agglomerated silicon powder

[***] Later referred to as *UConn*

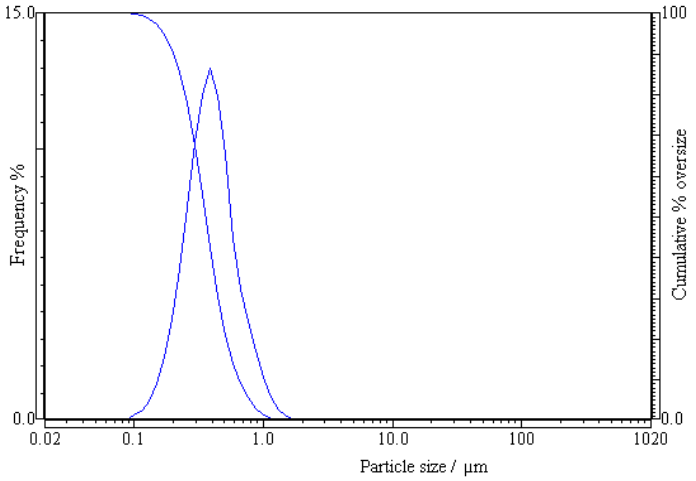

Figure 5. Particle size distribution present in milled silicon powder. Median particle diameter was 0.360 micron after a 15 h milling period (Attritor mill).

- ***Step 3:*** *Microwave field irradiation.* Graphite particles, along with the adsorbed hydrocarbon/silicon layer, were subjected to microwave irradiation at 500-1000 W power settings, for periods ranging from 1-60 minutes. Graphite is very efficiently heated in a microwave field, which would significantly facilitate our proposed synthesis method. The optimum power and time settings were to be established on the basis of physical characterization methods, as well as the electrochemical (coin half-cell) testing. We were hoping that this step would potentially generate the partially graphitized carbon that encapsulated the silicon nanoparticles.
- ***Step 4:*** *Carbon-coated product retrieval.* Silicon particles were dried and ground in a mortar.

1.3.4.2 Characterization of synthesized composite material

The synthesized graphite/nano-silicon/partly graphitized carbon composites were characterized first by physical methods (X-ray diffraction, scanning electron microscopy) and then in coin cells against lithium metal (half-cells) and against the standard $LiNi_{0.8}Co_{0.2}O_2$ cathodes (full cells). The capacity and the discharge/charge rate capability of the synthesized composite materials were compared against our standard electrodes (MCMB 6-28 carbonaceous anodes).

Task 3. Physical characterization of synthesized materials

The physical analyses results (XRD, SEM, particle size distribution) would help to establish the relationship between the physical properties of synthesized materials and their electrochemical performance. The scanning electron microscope (SEM) was used to examine the surface morphologies of synthesized materials.

Raman spectroscopy was used to characterize substrate particles prior to the synthesis, and the synthesized materials. Many properties of carbons (such as conductivity, lithium-ion intercalation capabilities) directly relate to the atomic bonding.[9,10] Graphite, amorphous carbons, and nanostructured carbon materials have been detected and analyzed by means of Raman spectroscopy.

Raman spectra of carbons consist, in most cases, of two prominent bands: one that is centered at ~1550 cm^{-1}, corresponding to sp^2-coordinated crystalline graphite, and another band at ~1350 cm^{-1}, attributed to the sp^3-coordinated disordered carbon.[11] The XRD, SEM, and Raman spectroscopy measurements will be performed at *UConn*. The results of physical characterization (X-ray diffraction, scanning electron microscopy, and particle size analyses) were correlated with the Li half-cells and full cells performance of synthesized materials.

Task 4. Preliminary Anode Coin Half-Cell Cycling

The electrochemical performance of the synthesized materials was first be evaluated in coin half-cells (Figure 6) at *Yardney Technical Products, Inc*. using a short cycling profile. The coin half cells, containing metallic lithium as the anode, were assembled under argon atmosphere inside a glove box. The cells will be filled with or standard electrolyte solution of 1.0 M $LiPF_6$ dissolved in a 1/1/1 EC/DMC/DEC mixture. The coin cells were cycled under constant current/constant voltage conditions to determine cell voltage, capacity, and the discharge/charge cycling efficiency of the synthesized anodes. The preliminary coin cells testing furnished information on anodes capacity and helped to select candidate materials for further studies.

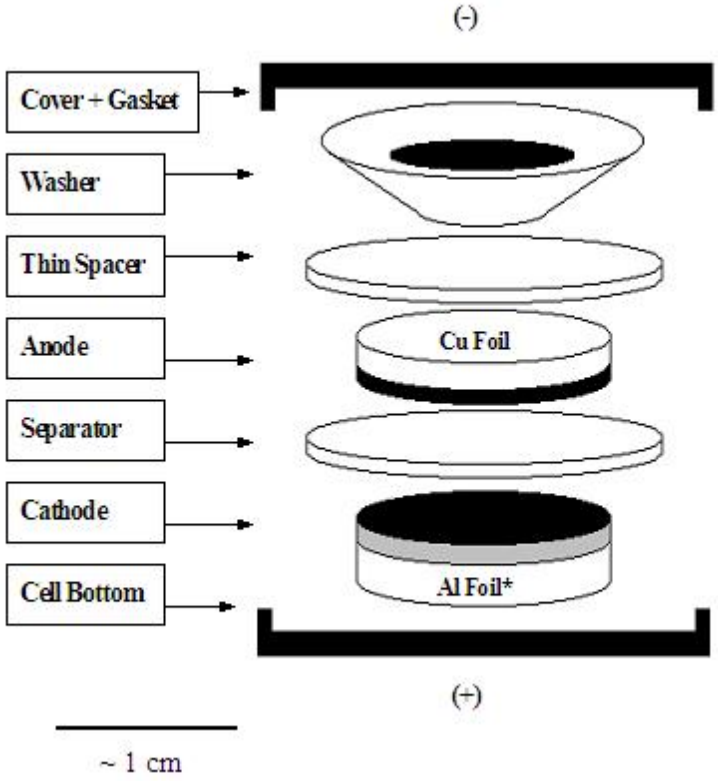

Figure 6. Coin cell assembly. In lithium half-cell, a lithium metal disc is used in place of aluminum foil-supported cathode.

The following short cycling profile was used to screen the synthesized anode materials:

1. 1 cycle (formation): **C/20** CC/CV (taper) charge and **C/20** discharge
2. 2 cycles: **C/10** CC/CV charge and **C/10** discharge
3. 3 cycles: **C/10** CC/CV charge and **C/5** discharge
4. 2 cycles: **C/10** CC/CV charge, **C/10** discharge

Task 5. Further Anode Coin Half-Cell Cycling

Practical aspects such as the best binder/active material ratio, and other electrode processing details needed for the in-depth full cell testing were evaluated in coin half-cells that were cycled according to the extended cycling profile:

5. 1 cycle (formation): **C/20** CC/CV (taper) charge and **C/20** discharge
6. 2 cycles: **C/10** CC/CV charge and **C/10** discharge
7. 3 cycles: **C/10** CC/CV charge and **C/5** discharge
8. 3 cycles: **C/10** CC/CV charge and **C/2** discharge
9. 3 cycles: **C/10** CC/CV charge and **C** discharge
10. 2 cycles: **C/20** CC/CV charge, **C/20** discharge

All half-cells were cycled within the 0.01-1.3V voltage range.

Task 6. In-Depth Full Coin Cell Cycling

Li-ion pouch full cells will be assembled at *Yardney* using C-silicon anode/Setela E20 Separator/ $LiNi_{0.8}Co_{0.2}O_2$ standard cathode. For electrolyte, 1 M $LiPF_6$ in the mixture of EC:DEC:DMC (1:1:1, vol.) will be used. The cycling profile for full cells will be basically identical to half-cell cycling profile in terms of cycling current rates. The full cells will be cycled within our standard cycling voltage range of 3.0 - 4.1V.

Prior to the assembly, the active electrode materials were coated onto the appropriate current collectors using standard techniques. Initial experiments used our standard electrolyte, 1 M $LiPF_6$ in the mixture of EC:DEC:DMC (1:1:1, vol.). Cell testing was performed at room temperature. Performance parameters that were compared included charge and discharge capacities and energies, cycle efficiency, and rate capability.

Task 7. Final Report Submittal

The final report, written jointly by *Yardney* and *the University of Connecticut* and provided to DoE, describes both the activities of the program and the findings of the experiments, performed in Tasks 1-6.

1.3.5 Research Findings or Results

1.3.5.1 CVD Carbon Coating Work done at the University of Connecticut

In this summary, the synthetic effort at the *University of Connecticut* is summarized. CVD apparatus (Figure 7) was used for coating silicon wafers with various crystallographic orientations while the coating parameters such as gases compositions, flow rates, temperature and reaction time were recorded.

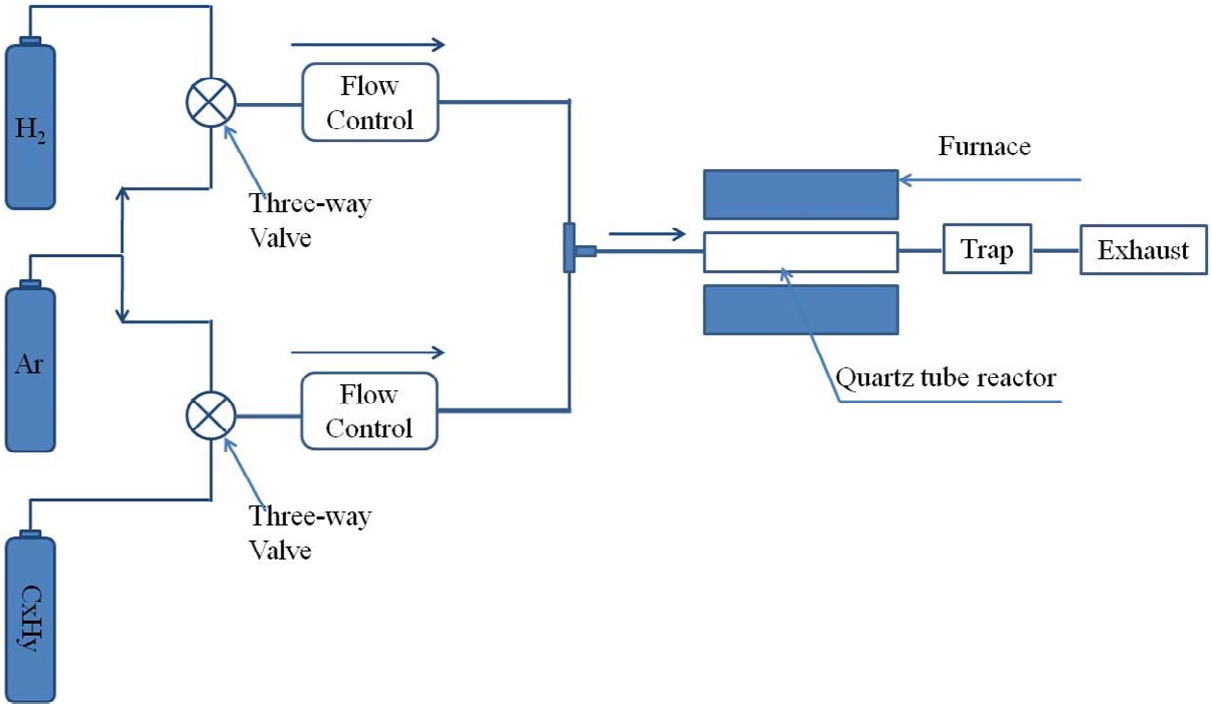

Figure 7. A schematic of the CVD apparatus at *University of Connecticut*

In this section, results of coating several samples are presented. The effect of the reaction time on carbon deposition from ethylene onto Si (111) wafers was explored in experiments LP19 and LP24. The impact of coating temperature with Si (111) was compared in samples: LP25, LP26 and LP28.

The influence of flow rate on coating quality and quantity was done on Si (111) in samples LP28 and LP30. For the effect of silicon wafers with different orientations, see the results of LP 30 and LP32 experiments. The impact of coating temperature at lower flow rate was investigated on Si (111), in samples LP30 and LP33 and the effect of ratio of C_xH_y to H_2 on Si (100) can be seen in samples LP32 and LP34. To investigate the impact of the carbon source, experiments LP30 and LP35 were done. Table 2 summarizes the synthetic parameters that were investigated during the course of this part of the Phase I project.

Table 2. Silicon wafer coating experiments done at University of Connecticut

ID	Silicon wafer	Carbon source	Ratio C_xH_y/H_2	Flow rate	Temperature / °C	Time / min	Characterization
LP19	Si(111)	C_2H_4	1:4	100:400	900	30	SEM, Raman
LP24	Si(111)	C_2H_4	1:4	100:400	900	120	SEM, Raman
LP25	Si(111)	C_2H_4	1:4	100:400	800	120	SEM, Raman
LP26	Si(111)	C_2H_4	1:4	100:400	850	120	SEM, Raman
LP28	Si(111)	C_2H_4	1:4	100:400	900	120	SEM, Raman
LP30	Si(111)	C_2H_4	1:4	50:200	900	120	SEM, Raman
LP32	Si(100)	C_2H_4	1:4	50:200	900	120	SEM, Raman
LP33	Si(111)	C_2H_4	1:4	50:200	850	120	SEM, Raman
LP34	Si(100)	C_2H_4	1:8	50:400	900	120	None
LP35*	Si(111)	CH_4	1:4	50:200	1000	120	---

*When CH_4 was used as carbon source, no coating could be obtained at this condition.

FE-SEM and Raman were used to investigate the quality of the coatings. Figure 8 shows the FE-SEM images of samples with different reaction time on Si (111). Carbons on Si (111) had spherical morphologies both on LP19 and LP24. Based on the images, with longer reaction times, more carbons deposition was observed on the silicon wafers. However, there was no obvious difference for the Raman shifts of the samples (see Figure 9). The two peaks around 1600 cm^{-1} and 1380 cm^{-1} are due to amorphous carbon.

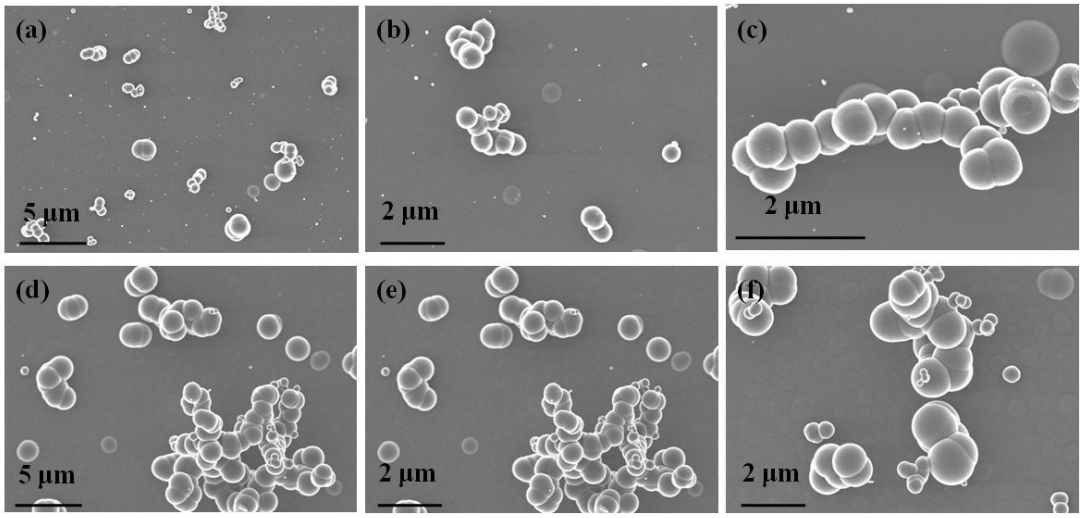

Figure 8. FE-SEM images of samples at different magnifications (a), (b) and (c) for LP19; (d), (e) for LP24

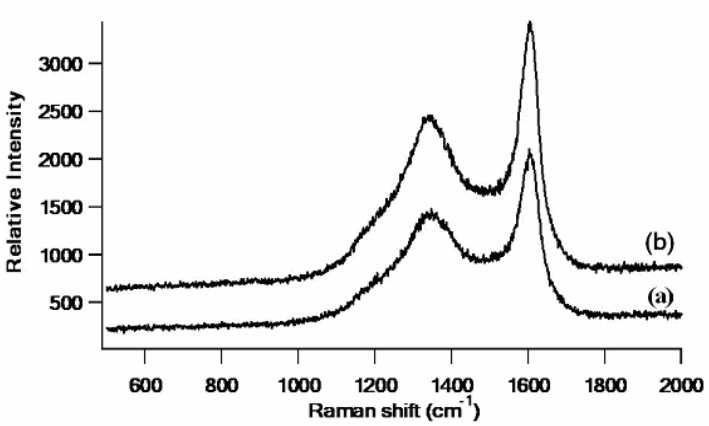

Figure 9. Raman spectra of samples: (a) LP19, and (b) LP24

Figure 10 shows the FE-SEM images of the coatings at different temperatures on Si (111). When the coating temperature was 800°C (sample LP25), some spherical carbon particles of carbon were obtained. As the temperature was increased to 850°C (sample LP26), more homogenous coatings were generated underneath the spherical particles of carbon. When the coating temperature was 900 °C (sample LP28), more spherical carbon coating were formed, and no other coatings were observed under the spheres. In the Raman spectra (Figure 11), no big differences, either in position or intensity was observed.

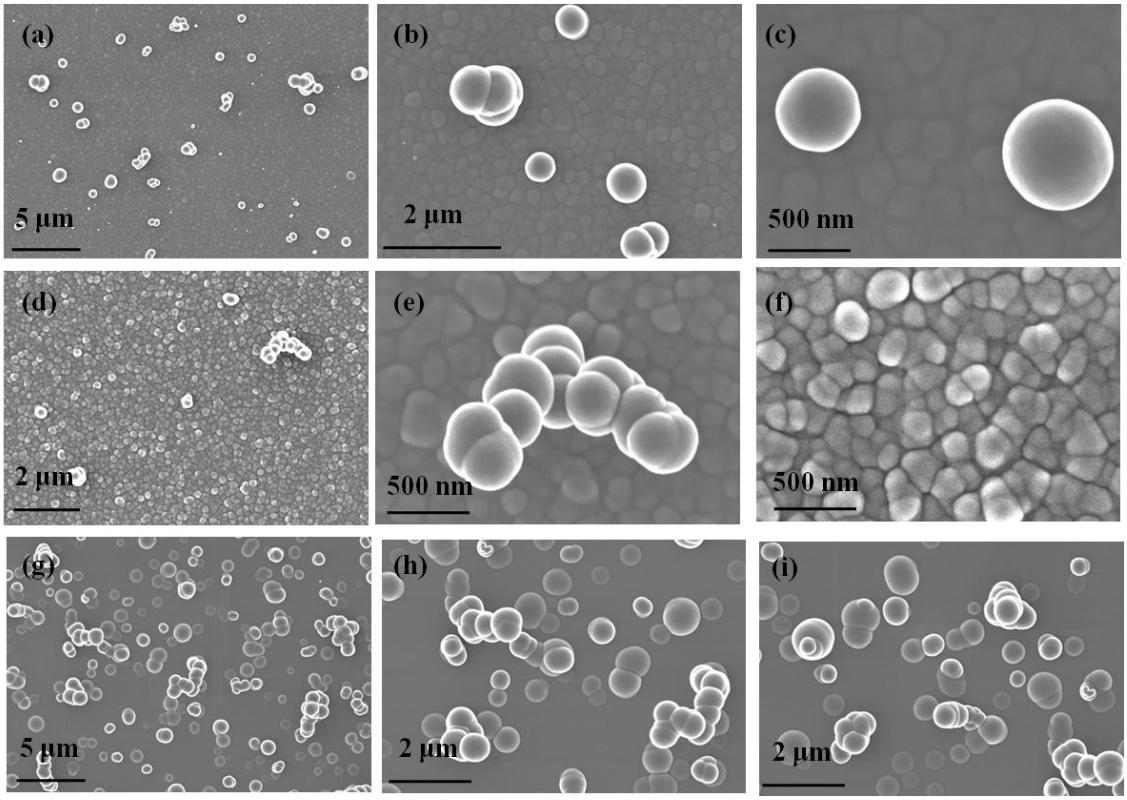

Figure 10. FE-SEM images of samples at different magnifications (a), (b) and (c) for LP25; (d), (e) and (f) for LP26; (g), (h) and (i) for LP28

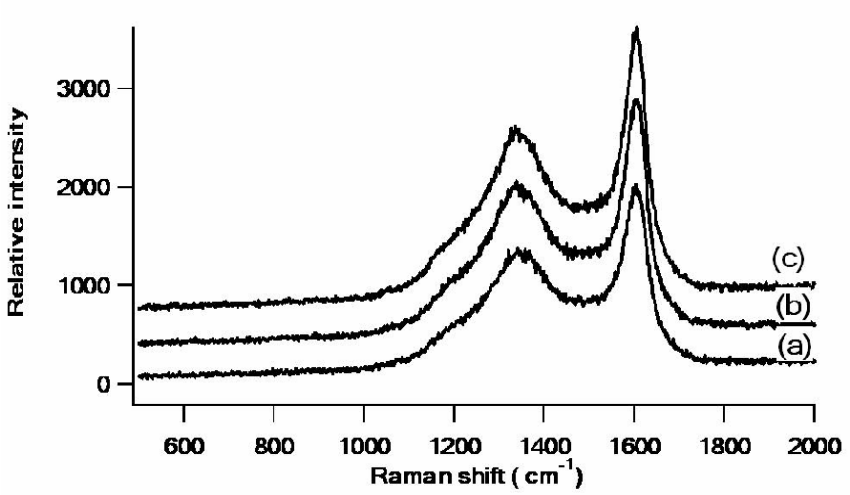

Figure 11. Raman spectra of samples: (a) LP25, and (b) LP26, and (c) LP28

Figure 12 shows the images of samples prepared under different gas flow rates. Other parameters were kept the same, only the flow rates of gases were changed from 500 mL/min (sample LP28) to 250 mL/ min (sample LP30). The images of the samples suggest that the coatings done at lower flow rates were much more uniform than that done at higher flow rates. All the surfaces of the silicon wafers were coated with carbon.

Flow rates clearly play important role in the production of homogeneous coatings. However, no significant differences were observed in the Raman spectra for these different conditions of coatings (Figure 13).

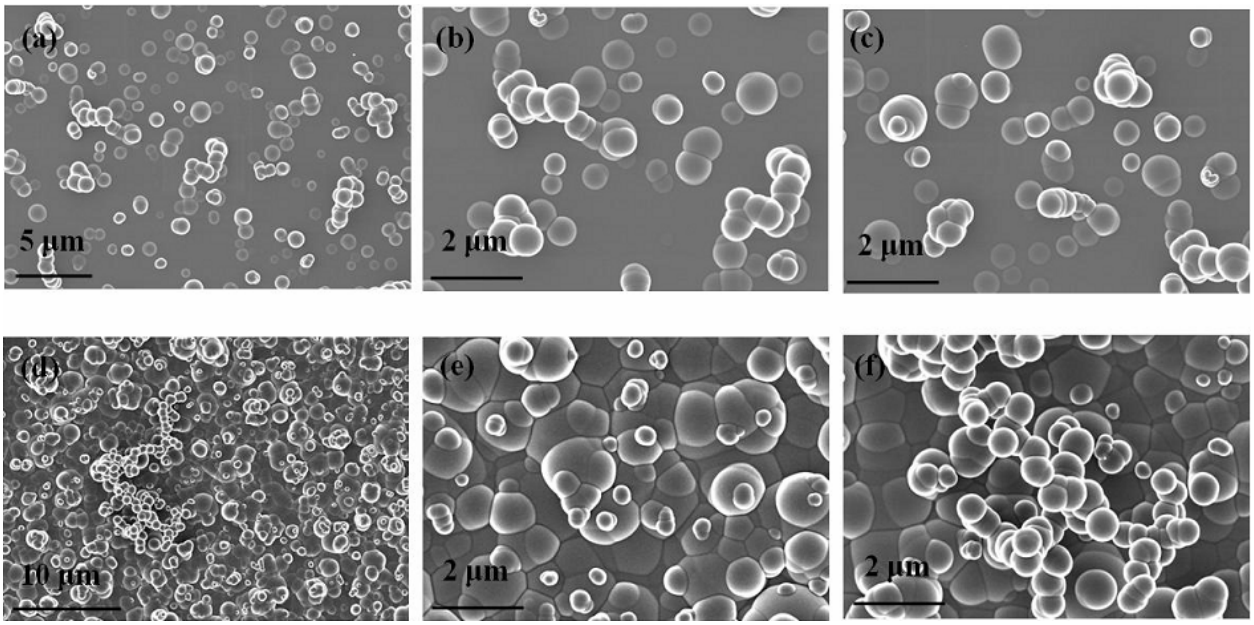

Figure 12. FE-SEM images of samples at different magnifications (a), (b) and (c) for LP28; (d), (e) and (f) for LP30

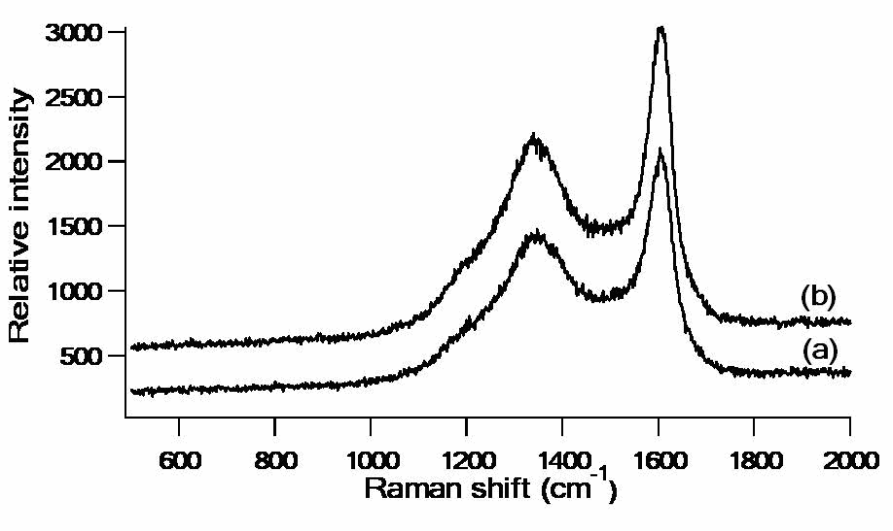

Figure 13. Raman spectra of samples: (a) LP28, and (b) LP30

The influence of silicon wafers with different orientations was studied, as shown in Figure 14 and Figure 15. With regard to the morphologies in Figure 14, the coatings on Si (111) - sample LP30 and Si (100) - sample LP32, did not show any significant differences. Raman spectra of the two coatings were the same (Figure 15). Therefore, under these conditions, the different orientations of silicon wafers did not markedly affect the coating.

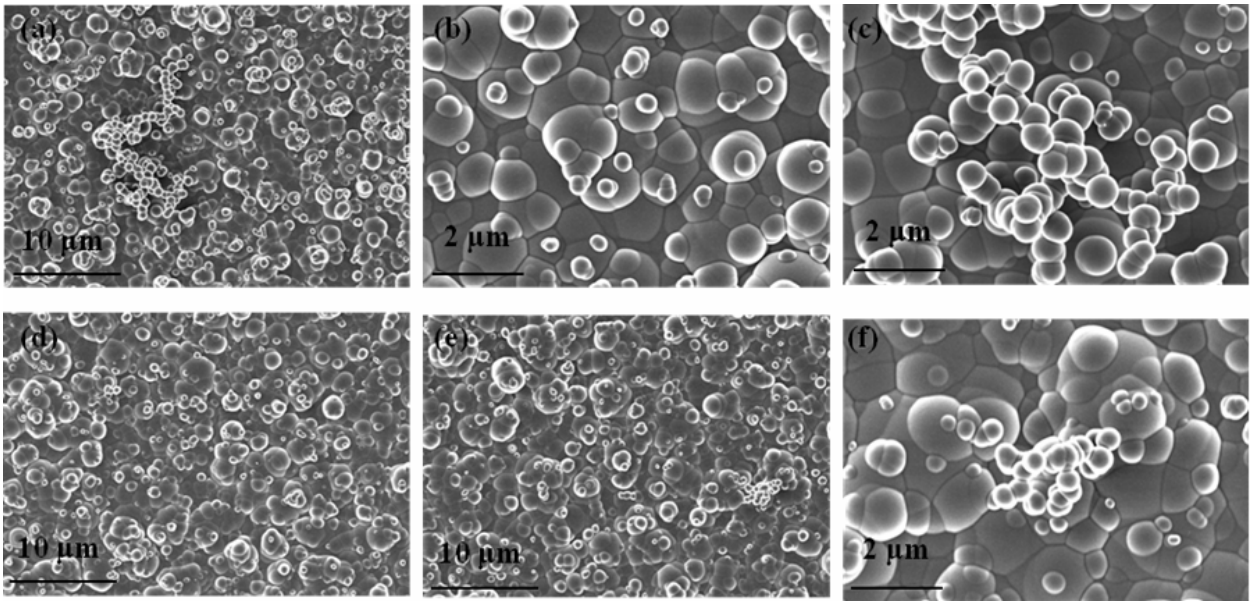

Figure 14. FE-SEM images of samples at different magnifications (a), (b) and (c) for LP30; (d), (e) and (f) for LP32

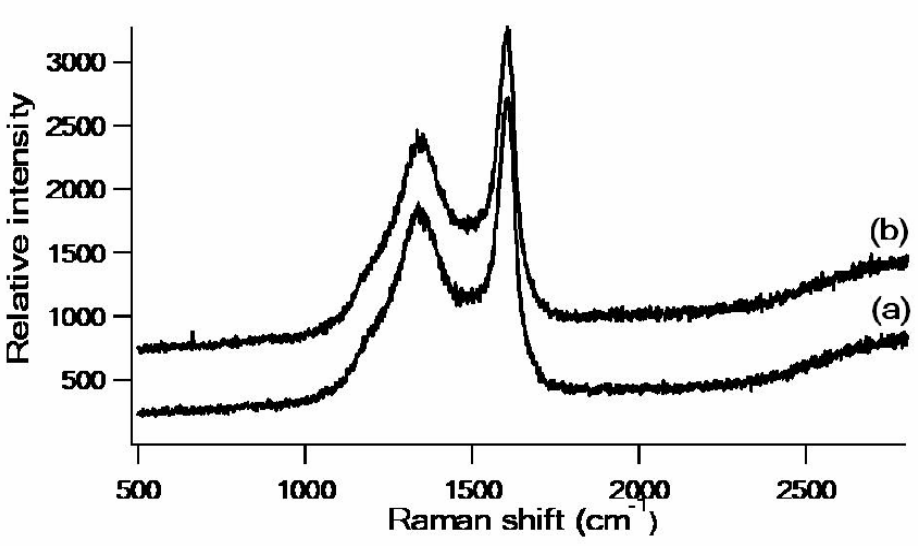

Figure 15. Raman spectra of samples (a) LP30, and (b) LP32

Based on the above comparisons, at higher flow rates, no matter which temperature was used, uniform coatings were not observed. Lower flow rates were favorable for homogeneous coatings, so the influence of temperature was investigated when lower flow rates were used in these systems. As shown in Figure 16, when the temperature was 850 °C (sample LP33), almost no coating was observed, only a very few spherical particles of carbon were found on the wafers. Accordingly, the intensity of Raman peaks for LP33 (Figure 17a) was much lower than the intensity of LP30 (Figure 17b).

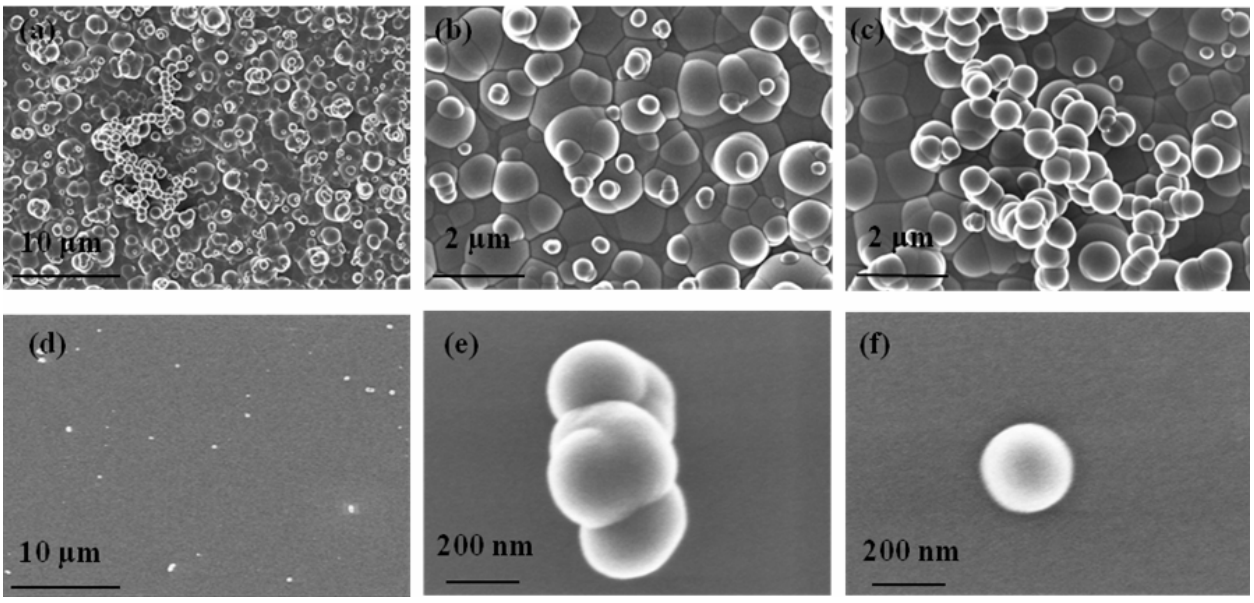

Figure 16. FE-SEM images of samples at different magnifications (a), (b) and (c) for LP30; (d), (e) and (f) for LP33

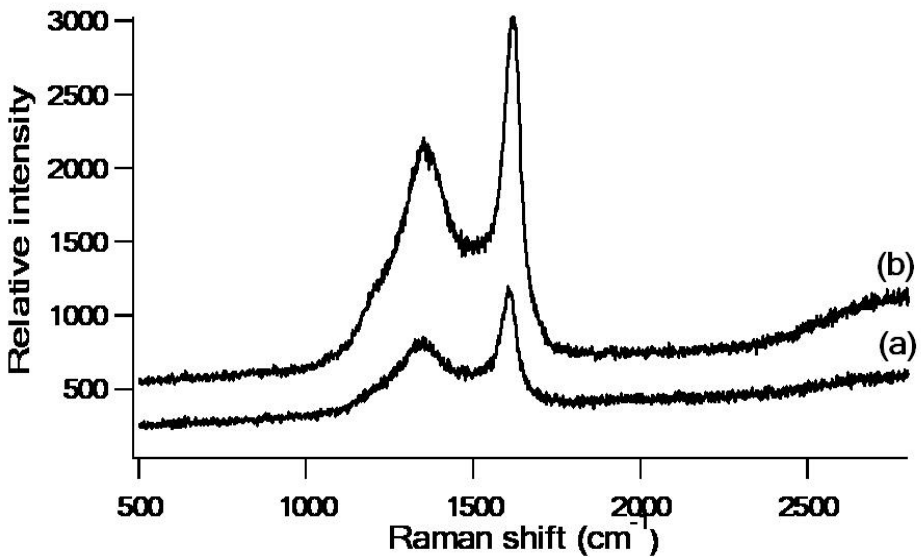

Figure 17. Raman spectra of samples (a) LP33, and (b) LP30

Methane (CH_4) did not work in our syntheses done at the selected set of parameters (Table 2). Propane (C_3H_8) may be used as alternative carbon source in the future. Detailed studies of the growth of carbon coatings on both Si (111) and Si (100) will be investigated with ethylene (C_2H_4) used as the carbon source.

1.3.5.2 Coin Cell Testing Done at Yardney Technical Products, Inc.

1.3.5.2.1 Preliminary Half-Coin Cells Testing

The initial synthetic activities at Yardney were related to Task 2: Microwave-assisted syntheses of graphite/silicon/carbon composite anode materials. However, upon encountering some technical difficulties with the reactant slurry transfer to the microwave reactor as well as c the subsequent the accelerated evaporation of hydrocarbon precursors, we have decided to coat the silicon powders with amorphous carbon via vapor deposition (CVD) first and then expose the carbonaceous coatings to microwave field. Our decision was reinforced upon observation of non-uniform coating from the slurry-based delivery.

The testing of non-uniformly (even upon a visual inspection) samples confirmed that those samples were not coated successfully – preliminary coin cells (not shown her) failed in a similar manner to an uncoated reference sample shown in Figure 18. Sample DT2ua shown in the figure was done as a baseline of the un-coated silicon powder. The following anode composition was used in the test half-cell: 87 wt% per solids of active material (silicon powder, attritor-milled to about 300-400 nm, uncoated), 9.9 wt% pVdF binder, 0.1 wt% bonding agent (Pelmore™ catalyst) and 3 wt% of conductive carbon diluent (SuperP carbon).

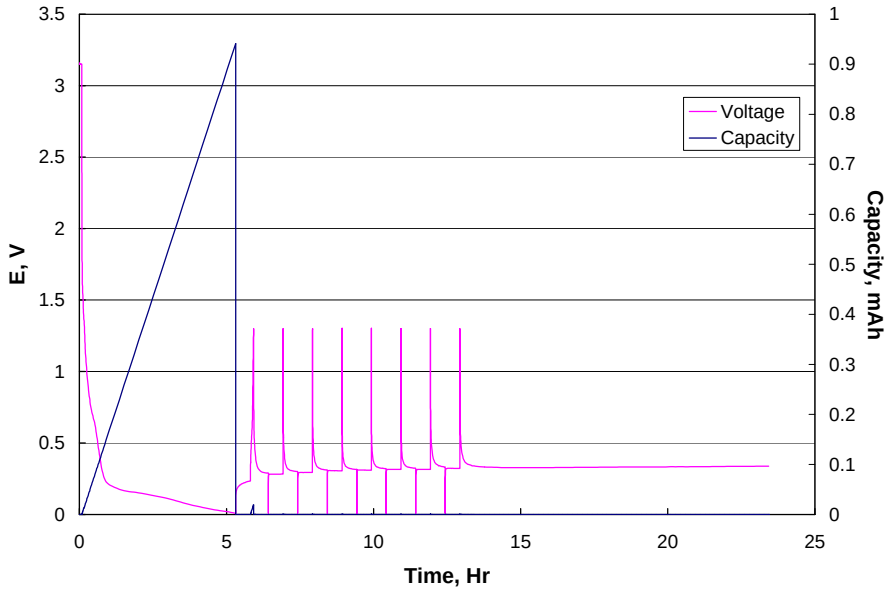

Figure 18. Potential vs. time and capacity vs. time for (failed) cell DT2ua

A similar composition coating of the physical mixture of the graphitic carbon with silicon powders (sample batch DT3u) also did not succeed in coin cell preliminary testing (not shown here, similar to DT2u data). However, we produced our first viable sample when we decided to coat the silicon powders by the chemical vapor deposition (CVD) route. See Figure 19 and Figure 20 for the preliminary half-coin cell testing results for this sample.

The first successfully cycled sample batch was denoted DT7 and the syntheses were performed as follows: the milled silicon nanoparticles with about 300-400 nm particle size (*Union Process*, Chicago, IL) were placed in the CVD reactor. Carbon coating was deposited from toluene that was placed in the bubbler with argon gas (*Airgas*) flowing through and carrying toluene vapor to the heated CVD reactor.

The powder substrate was pre-heated prior and during the carbon deposition in a high-temperature furnace at 900ºC. A schematic of the used CVD reactor was similar to that shown in Figure 3. DT7 electrode composition in the half-coin cell was: 87 wt% CVD-coated silicon, 9.9 wt% pVdF binder, 0.1 wt% bonding agent (Pelmore™ catalyst) and 3 wt% of conductive carbon diluent (SuperP carbon).

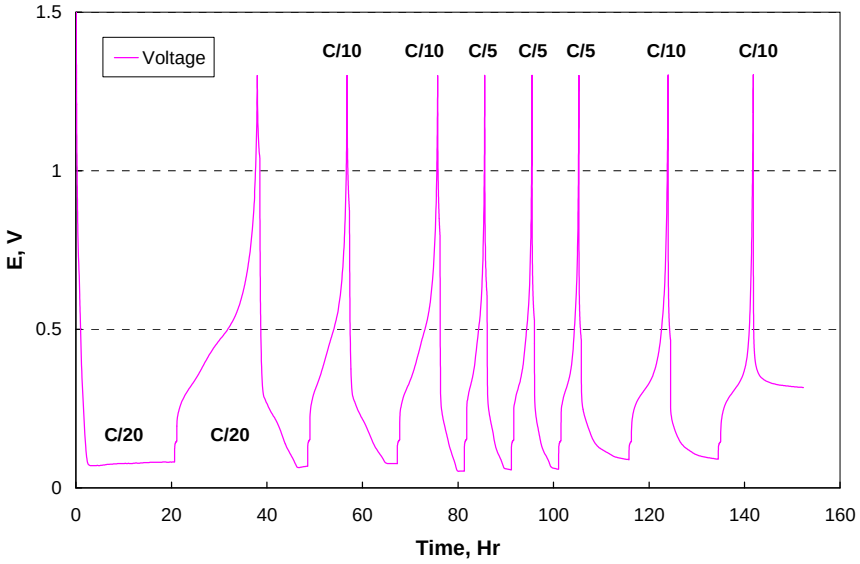

Figure 19. Potential vs. time for cell DT7b

The Figure 20 illustrates that sample DT7 cycled within the proper 0.01-1.3V voltage range (Figure 19) and had considerable discharge capacity (in the half-cell this means lithium-ion insertion into the anode structure), but the charge capacity slowly faltered and not all inserted lithium-ions left the silicon-based anode. This accumulation of Li-ions persisted throughout the entire DT7 testing regimen.

The irreversible lithium-ions retention occurs commonly in the first cycles of testing the carbon-based anodes; however in silicon anodes this seems to be a more pronounced and persistent phenomenon. In carbon-based anodes, the first cycle usually suffers from some 10-15% irreversible capacity loss but the discharge/charge capacity ratio improves in the subsequent cycles. Insufficient electronic conductivity of silicon and/or the lack of sustained electrical contact of active material with the current collector could be the causes for this slow capacity fade.

Another coating formulation (DT9, see Figure 21) was based on the same coated material that DT7 (Figure 20) and was prepared in order to test the hypothesis that in the increased electronic conductivity environment and with improved electrical current collection, the lithium-ion retention within silicon anode in later cycles should subside. Some irreversible capacity (about 10-15%) on the first cycle would be still expected due to the anode formation process which in normal conditions consumes lithium. However, the subsequent cycles discharge/charge ratios should improve. This was, in fact, confirmed in sample batch DT9.

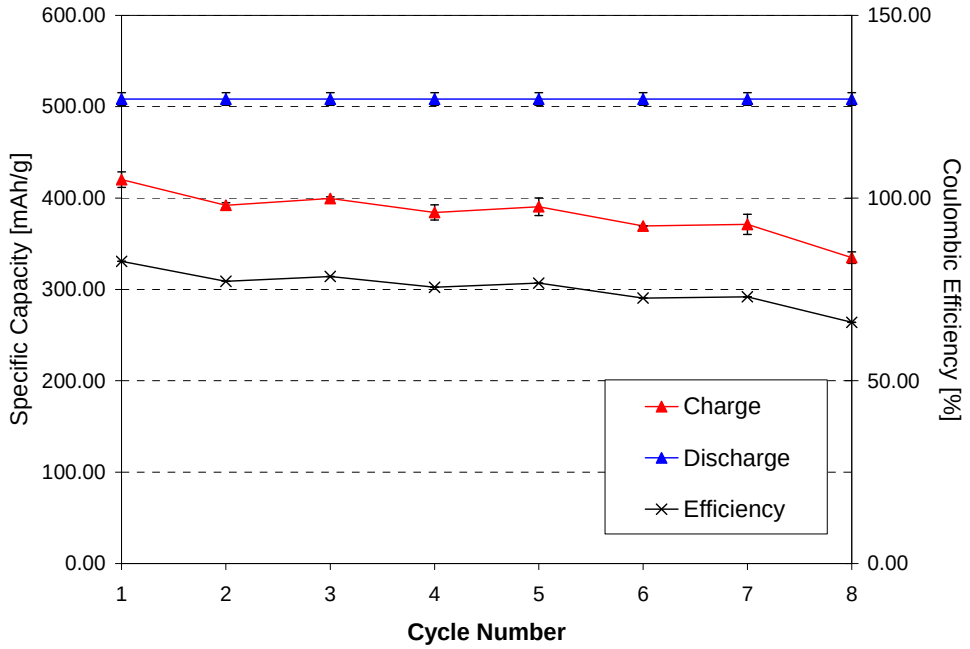

Figure 20. Specific capacity vs. cycle number plotted for coin half-cell batch DT7

The coin half-cell batch DT9 shown in Figure 21 was based on the silicon-carbon anode (same active powder as DT7) with the following composition: 57 wt% CVD-coated silicon, 30.9 wt% pVdF binder, 0.1 wt% bonding agent (Pelmore™ catalyst) and 12 wt% of conductive carbon diluent (SuperP carbon). This conductive diluent-rich environment with enhanced adhesion to copper current collector indeed improved the charge/discharge ratio on the second and further cycles.

Even though the 57 wt% active formulation is not practical for the real-life lithium-ion battery due to the low energy density, the DT7-DT9 comparison points to the importance of development activities focused on the proper binder selection. Part of the enhanced charge capacity could be caused by the reasonably large addition of conductive diluents, like SuperP or acetylene black carbons. The exact contribution of the increased binder and diluents contributions is currently not resolved and should be pursued in the future research.

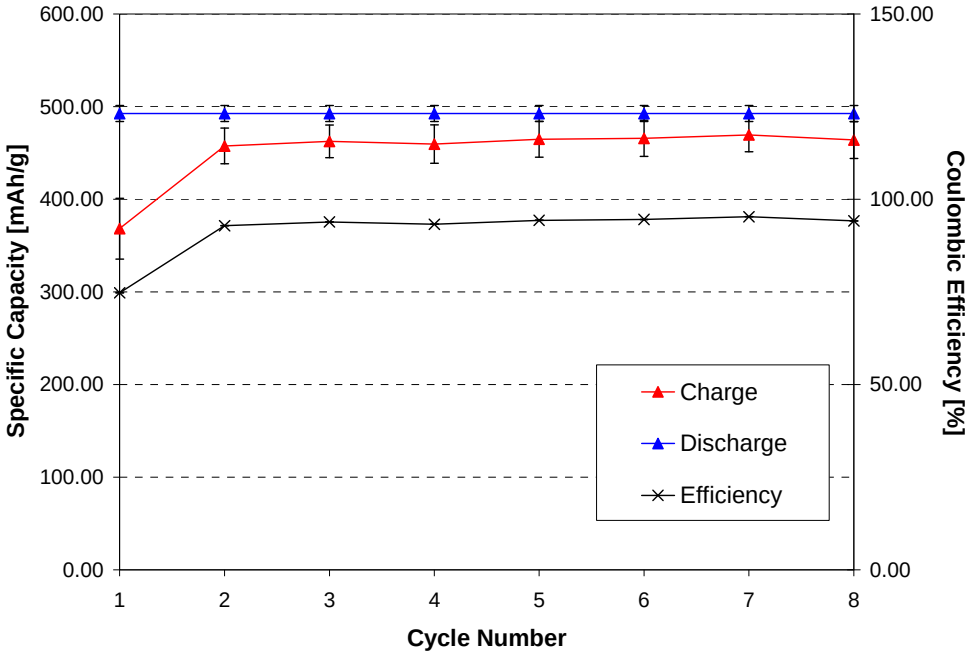

Figure 21. Specific capacity vs. cycle number plotted for coin half-cell batch DT9, capacity cut-off was at 500 mAh/g. Average of three cells was taken, error bars are based on the standard deviation value within the series.

Encouraged by the success of the CVD carbon deposition method in producing a well-performing electrode material, we have decided to post-process the CVD-carbon coated silicon powders by exposing them to microwave field. Thus, samples DT14 and DT18 were prepared. The cycling results for cell batch DT18 are shown in Figure 22.

Samples DT14 and DT18 were prepared in the following manner: silicon particles that already underwent the CVD carbon coating process (same as samples DT7 and DT9) were placed in the quartz reactor which was then pumped down to about 10 Torr vacuum. The silicon substrates were then subjected to microwave irradiation at 500-1000 W power settings, for 60 minutes.

For the future experiments with MW-assisted coating optimum power and time settings will be established on the basis of physical characterization methods. The future power and temperature and time parameters in MW-assisted experiments will most likely be lower (power and/or temperature), and shorter (MW-exposure time). We were hoping that this step would potentially generate the partially graphitized carbon that encapsulated the silicon nanoparticles. Based on the cycling results of samples DT18 shown in Figure 22 we suspect the somewhat arbitrarily set initial microwave treatment conditions were too “harsh” and some surface reaction between the silicon powder and deposited carbon may have occurred, maybe even producing a thin layer of silicon carbide-like layer.

The SiC formation hypothesis needs to be confirmed or disproved by X-Ray diffraction and Raman spectroscopy results but some preliminary observations including the observed increased "hardness" of the DT18 powders (the DT18 powders were much more difficult to grind in a mortar than samples DT7 or DT9 and the assembled DT18 full cells needed thicker separator than the normally used 20-micron thick Setela separator (the DT 18 full cells results are presented later in this report, see Figure 24). The half-coin cells results of DT18 cycling Figure 22 confirm that the material quality and electrochemical performance actually decreased upon the prolonged exposure to the microwave field. Therefore, in the full cells testing that is presented in later sections of this report, DT9 anode plates were used in cell assembly since this electrode is the best-performing silicon-carbon composite material to date.

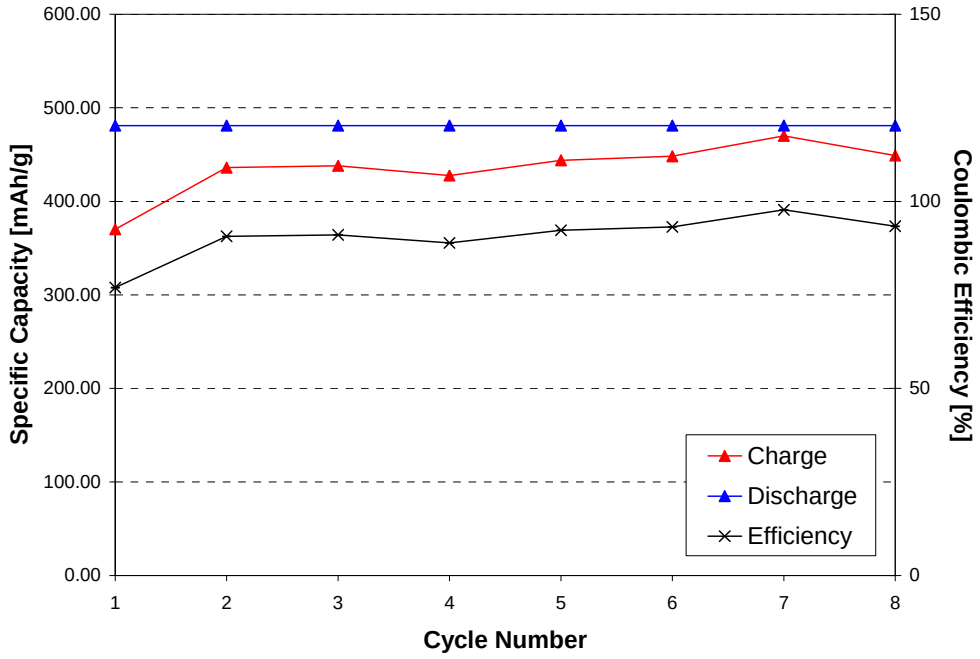

Figure 22. Specific capacity vs. cycle number plotted for coin half-cell DT18b, capacity cut-off was at 500 mAh/g

1.3.5.2.2 In-Depth Half-Coin and Full Coin Cell Testing

This section summarizes the continued testing of the most promising anode materials in coin full cells compared to our "baseline" meso-carbon micro bead (MCMB) anodes. Electrodes identical to DT9 were selected for the expanded coin cell testing. The DT9 electrodes contain the CVD-coated silicon powders (57 wt%), 30.9 wt% pVdF binder, 0.1 wt% bonding agent (Pelmore™ catalyst) and 12 wt% of conductive carbon diluent (SuperP carbon).

Figure 23 shows the results of our synthesized DT9 anode cycling against one of the *Yardney's* "standard" cathode formulations based on the $LiNi_{0.8}Co_{0.2}O_2$ material (red line for charge, blue line for discharge). The DT9 results were with our "baseline" chemistry (MCMB-type anode vs. $LiNi_{0.8}Co_{0.2}O_2$ cathode (pink line for charge, black line for discharge). In both cases, same cathode lot was used (*Yardney* cathode lot#6034-1).

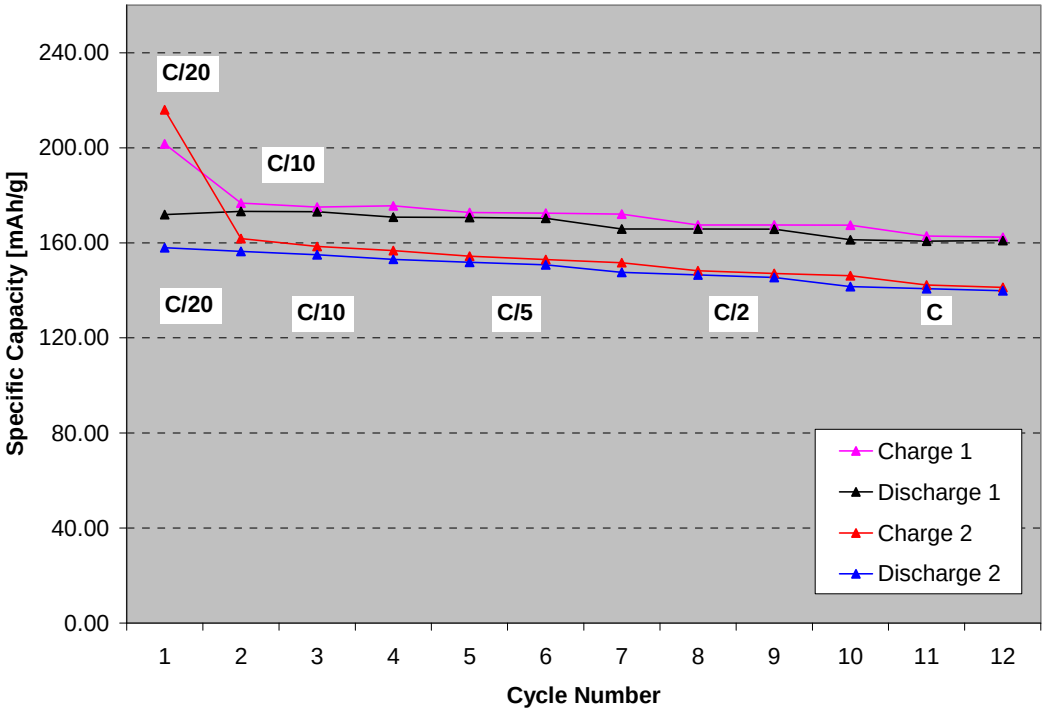

Figure 23. Full coin cell series with carbon-coated silicon-based anode (DT9) vs. $LiNiCoO_2$ cathode (lot 6034-1) compared to a full cell (large size, 7-Ah), also with the 6034-1 cathode vs. "standard" MCMB anode

One can see in Figure 23 that the reversible capacity value on the first cycle of DT9 vs. lot 6034-1 was about 73% which is lower than a typical value of about 85% for the commercial MCMB carbon-based anodes. Two factors could contribute to this high irreversible capacity values in silicon powder anodes:

- The Si powders have particle size range of 300-400 nm and their surface area would be higher than the 6 or 10 micron MCMB carbon anodes.
- The cathode/anode ratio was not optimized in this experiment. Usually in our silicon testing experiments, we used the capacity cut-off value of 500 mAh/g for all Si/C anodes. This assumption would need to be validated and the optimal cathode/anode ratio needs to be established. In the proposed Phase II work section we suggest the utilization of a new testing cell for the cathode/anode balancing experiments.

The following graph, shown in Figure 24 adds another testing cells batch to the comparison of the DT9 full cells and "baseline" full cells that were shown above in Figure 23: the new line (green for charge, purple for discharge) represents DT18 materials in full cells vs. the $LiNi_{0.8}Co_{0.2}O_2$ cathode. As it was mentioned before, in the preliminary half-cell section, thicker separator was used instead of the 20-micron Setela separator (that was used in all other cells). It is clear from this comparison graph that the MW-treated sample was over-exposed to microwaves and some unfavorable changes occurred in the cathode material.

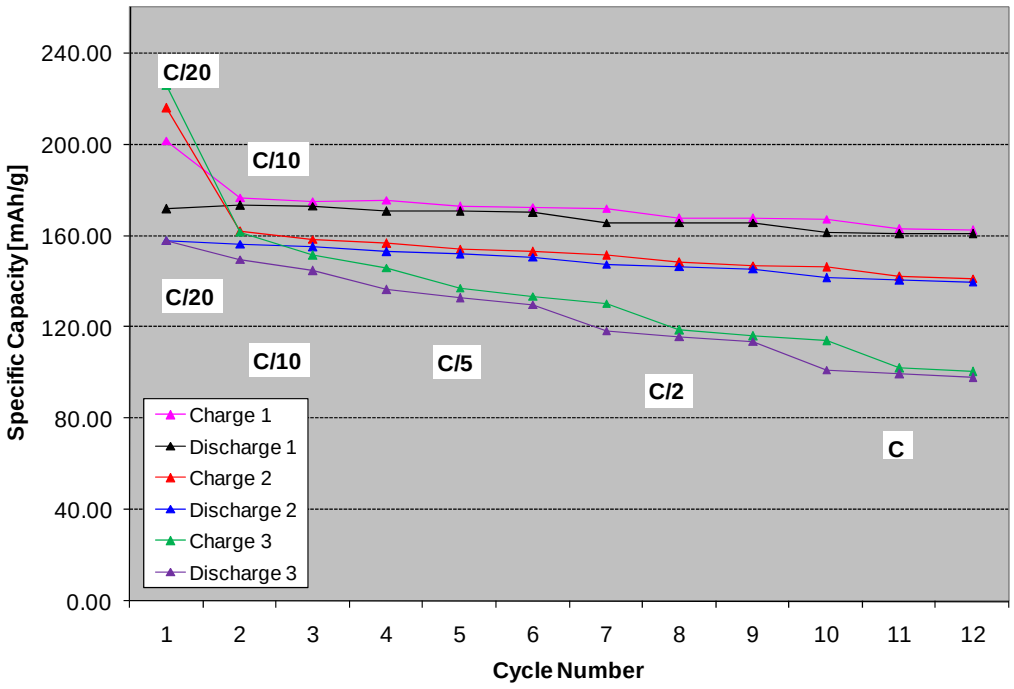

Figure 24. Full coin cell series with carbon-coated silicon-based anode (DT9) vs. $LiNiCoO_2$ cathode (6034-1) - middle line, compared to our "baseline" cell chemistry (top line) and DT18 anode vs. $LiNiCoO_2$ cathode (bottom line).

1.3.6 Our Estimate of Technical Feasibility

In the following section we will respond to the technical questions that we formulated at the beginning of this project in hope of a better understanding of the C/Si materials. We will also discuss the degree to which the technical objectives were met and the degree of success of various technical tasks that we have accomplished in the Phase I.

1.3.6.1 Technical Questions to be answered in the Phase I

At the beginning of the Phase I research we have formulated several technical questions that would help us to address the technical objectives defined for this program. In this section we present the technical questions, followed by the related findings of this Phase I effort.

Question 1: Which synthetic method yields the most continuous, thin carbon coating?

Scanning electron microscopy (SEM) was the characterization method that was used to find an answer to this question. Chemical vapor deposition methods seem to yield the most continuous and the most uniform carbon coatings to date.

Question 2: Which synthetic method yields a C-nano-Si anode composite with the best electronic conductivity?

From the coin cells cycling we conclude that CVD yielded the most conductive Si/C material to date.

Question 3: To what extent can we decrease the conductive additive by using the C-nano-Si anode composite material?

This question was not answered yet. We are convinced that focused development efforts in Phase II effort are needed to optimize the electrode composition (e.g.: conductive diluents, binders used in the electrode formulation).

Questions 4 and 5: Will the rate capability improvement be observed upon decreasing the average particle size of the silicon component in composite materials? How to best utilize the C-nano-Si anodes in a practical lithium-ion battery?

Pouch cell and 7Ah cell cycling experiments will be used to obtain an answer to these questions in the proposed Phase II of this project. Advanced, cost-effective current collectors, electrolytes, binders, anodes etc. will be pursued as a part of the Phase II approach, based on the current *DoE* guidelines.

1.3.7 The Degree to which Phase I Objectives have been met

The purpose of this Phase I effort was to demonstrate feasibility of the silicon-carbon in lithium-ion batteries (LIB). We believe that this purpose has been met. More work is, by all means, necessary, but we believe that a good foundation for the Phase II effort was laid. The following technical objectives have been identified to meet the Phase I goals:

Objective 1. ***Prepare graphite/silicon/carbon composite anode materials***

Several experimental anode materials were synthesized and tested. While their electrochemical performance was not ideal, we believe that they could be optimized.

Objective 2. ***Characterize synthesized anode materials***

The synthesized anode materials and silicon wafers for coating parameters study were characterized by scanning electron microscopy, and Raman spectroscopy methods. Some XRD diffraction patterns were also taken (this information was not included here).

Objective 3. ***Test and evaluate performance of the anodes in half-cells and full cells***

The synthesized anode materials were tested in coin half-cells and full coin cells.

Objective 4. ***Correlate performance to matrix graphitization degree, silicon nanoparticle content and conductivity and screen the best active material candidates***

This part of research effort was partially fulfilled and more experiments were planned for the anticipated Phase II effort.

2. Bibliography and References Cited

[1] B. A. Boukamp, G. C. Lesh, R. A. Huggins, *J. Electrochem. Soc*., **128** (1981) 725.
[2] J. Wolfenstine, *Journal of Power Sources*, **79** (1999) 111.
[3] H. Ikeda, M. Fujimoto, S. Fujitani, M. Shima, H. Yagi, H. Tarui, H. Kurokawa, K. Asaoka, S. Matsuda, Y. Domoto, R. Ohshita, Y. Kato, H. Nakajima, T. Yoshida, Sanyo Electric Co., Ltd., Japan, *PCT Int. Appl*., WO 2001029918 (2001).
[4] M. Marcinek and R. Kostecki, *Proceedings of the 208th Electrochemical Society Meeting*, Los Angeles, CA October 2005, abstract number 114.
[5] F. S. Galasso, "*Chemical Vapor Deposited Materials"*, CRC press, Boca Raton, (1991).
[6] M. Marcinek and R. Kostecki, *Proceedings of the 208th Electrochemical Society Meeting*, Los Angeles, CA October 2005, abstract number 114.
[7] D. J. Shanefield, *Organic Additives and Ceramic Processing*, Kluwer Academic Publishers, Boston, London (1995).
[8] *Metals Handbook* Ninth Edition, **7**, *Amer. Soc. for Met*., Metals Park, Ohio (1984).
[9] A. C. Ferrari, J. Robertson, *Phys. Rev. B*, **61**, (2000) 14095.
[10] A. C. Ferrari, J. Robertson, *Phys. Rev. B*, **64**, (2001) 075414.
[11] P. C. Eklund, J. M. Holden, R. A. Jishi, *Carbon*, **33** (1995) 959.